Progress In Electromagnetics Research M, Vol. 39, 53–63, 2014

Pattern Synthesis for Large Planar Arrays Using a Modified Alternating Projection Method in an Affine Coordinate System

Dan Hua*, Wentao Li, and Xiaowei Shi

Abstract—A pattern synthesis approach based on a modified alternating projection method in an affine coordinate system is proposed in this paper. The approach is suitable for large planar arrays with skewed element layout. According to the affine transformation theory, the radiation pattern of the array with a periodic parallelogram element layout could be written down immediately from that of a conventional one with rectangle cells when a pattern invariant group is defined. Just as known, the conventional alternating projection method is sensitive to the starting point and easy to fall into local optimum; in this paper we introduce a modified alternating projection method with a variable projection operator. To verify the rationality of the proposed method, several examples have been performed on our personal computer. Results show that the method could quickly synthesize the array patterns to the required with high accuracy. In addition, if the array has a triangle or parallelogram element layout, the required antennas to fill up the aperture is reduced when compared with the conventional one with antennas arranged along a rectangle grid. In our examples, the maximum reduction is about 18.09%, which is quite beneficial to reduce the weight and cost of the array.

1. INTRODUCTION

In the design of large aperture antenna arrays, the number of antenna elements, phase shifters and other associate components becomes extremely large. Sometimes, to reduce the weight and cost and not to sacrifice the aperture gain, antennas are placed farther apart to fill up the same aperture. Ordinarily, in large phased arrays, antennas are arranged with element spacing equal to or less than a certain value which is determined by the main beam peak to suppress the generation of grating lobes. For example, in the case of full scan, the maximum element spacing is half the wavelength if the array has elements located on a rectangle grid. However, if the array has elements located along a parallelogram grid, the element spacing could be a little larger, and thus fewer elements would be required to fill up the same aperture [1]. In general, the array with an equilateral triangle element distribution could have a 13.4% reduction in the element number [2].

Evolutionary optimization algorithms, such as genetic algorithm (GA) [3, 4], particle swarm optimization (PSO) method [5, 6] and some hybrid methods [7, 8], have been successfully applied to synthesize array patterns to the required. However, the involved computation time to good result is always measured in hours or even days and/or the array size is not too large. In recent years, an iterative method based on the fast Fourier technique [9–12] was put forward to synthesize large planar arrays with uniform element spacings. In papers [9, 10], an affine transformation was applied on arrays with a triangular grid in order to get arrays with square element grid on which the standard IFT method could be applied on arrays featuring skewed grids. Further explanation is, a new coordinate system was obtained by making the column and row spacing equal through scaling, followed by a rotation of

Received 21 July 2014, Accepted 19 September 2014, Scheduled 6 October 2014

* Corresponding author: Dan Hua (hd19901002@126.com).

The authors are with the Science and Technology on Antenna and Microwave Laboratory, Xidian University, Xi'an, Shaanxi 710071, China.

the aperture x-y coordinate system over an angle of 45 degrees. In this rotated coordinate system, the elements are arranged along a square grid allowing the use of inverse and direct FFTs. In both papers, the far field of the arrays with a triangular grid was calculated in a very fast way using a proprietary method based on a chirp z-transform.

Generality, effectiveness and simplicity in the implementation explain the use of alternating projection method in array pattern synthesis [13–18]. Based on the concept of the projection, two sets are defined: one is the feasible set, and the other is the specification set. The former contains all the patterns that can be achieved, and the latter contains all the patterns that want to be obtained. An intersection of the two sets is a solution to the synthesis. The method is simple, fast and easy to implement on software. Moreover, alternating projection method is older than those methods including GA, PSO and IFT. While on the negative side, it is easy to fall into local optimum, which has motivated various modifications on the conventional method [15–17].

In this paper, we present a fast pattern synthesis approach for large periodic planar arrays. The approach is based on a modified alternating projection method in an affine coordinate system. The approach is capable of synthesizing any type of pattern, such as sum, different and shaped beams. When the array has a skewed lattice, the array factor could be quickly calculated by the inverse discrete Fourier transform if a special set of wavenumber vectors in an affine coordinate system is selected. After obtain the array pattern and compare it with the prescribed target, the samples which exceed the pattern limitations are altered with a modified projection operator, and then a new set of element excitations could be obtained by inversely projecting the modified pattern onto the feasible set. The procedure of the approach is shown as follows.

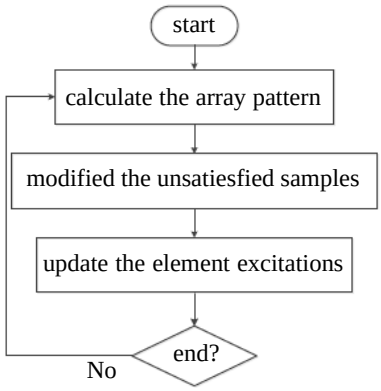

This iterative synthesis process continues until the pattern satisfies the requirements completely or the iteration reaches its maximum number.

The paper is organized as follows. Section 2 introduces the formulation of the array factor for arrays with periodic element layouts. Section 3 describes the synthesis approach. Section 4 presents several synthesis examples. Section 5 is the conclusion.

2. FORMULATION

Consider a general periodic array with elements distributed along a skewed grid. For simplicity, let one side of the parallelogram parallel to x-axis in the xoy plane as shown in Figure 1.

The element position vector $\overrightarrow{r_{mn}}$ equals

$$\overrightarrow{r_{mn}} = m\overrightarrow{d_1} + n\overrightarrow{d_2}; \quad 0 \le m \le M-1, \quad 0 \le n \le N-1 \tag{1}$$

where $\overrightarrow{d_1}$, $\overrightarrow{d_2}$ are the periodic vectors along the lattice, and M, N are the total element number along the directions $\overrightarrow{d_1}$ and $\overrightarrow{d_2}$, respectively. The array factor F_a can be written as

$$F_a\left(\vec{k}\right) = \sum_{m=0}^{M-1}\sum_{n=0}^{N-1} I_{mn} \cdot e^{j\left[m\left(\vec{k}\cdot\overrightarrow{d_1}\right)+n\left(\vec{k}\cdot\overrightarrow{d_2}\right)\right]} \tag{2}$$

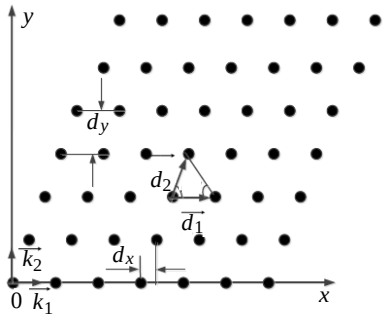

Figure 1. Parallelogram element lattice.

where I_{mn} is the aperture current distribution, $\vec{k}$ the wavenumber vector, and

$$\vec{k} = k_x\hat{x} + k_y\hat{y} = 2\pi/\lambda \cdot (u\hat{x} + v\hat{y})\,; \quad \overrightarrow{d_1} = d_1\hat{d}_1; \quad \overrightarrow{d_2} = d_2\hat{d}_2 \tag{3}$$

Obviously, although a vector may be fixed in space, its components are mutative depending on the bases of the coordinate systems. Let

$$\vec{k} = k_x\hat{x} + k_y\hat{y} = k_1\hat{k}_1 + k_2\hat{k}_2 \quad \left(\hat{k}_1 \neq \hat{k}_2\right) \tag{4}$$

where $\hat{k}_1$, $\hat{k}_2$ are arbitrary unit vectors in wavenumber space. To take advantage of the efficiency of DFT/IDFT, let

$$\hat{k}_1 \cdot \hat{d}_2 = 0 \quad \text{and} \quad \hat{k}_2 \cdot \hat{d}_1 = 0 \tag{5}$$

the array factor (2) then can be further expressed as

$$F_a\left(k_1, k_2\right) = \sum_{m=0}^{M-1}\sum_{n=0}^{N-1} I_{mn} \cdot e^{j\left(mk_1d_1\hat{k}_1\cdot\hat{d}_1 + nk_2d_2\hat{k}_2\cdot\hat{d}_2\right)} \tag{6}$$

Equation (6) is the formulation of the array factor for periodic planar array with parallelogram element layout. As a special case, when the array has a rectangle element layout, there is

$$d_1 = d_x; \quad d_2 = d_y; \quad k_1 = 2\pi u/\lambda; \quad k_2 = 2\pi v/\lambda; \quad \hat{k}_1 = \hat{d}_1 = \hat{x}; \quad \hat{k}_2 = \hat{d}_2 = \hat{y} \tag{7}$$

3. DESCRIPTION OF THE METHOD

Consider a finite two-dimensional sequence $x(m, n)$. Its discrete Fourier transform (DFT) can be written as

$$X\left(k, l\right) = \sum_{m=0}^{M-1}\sum_{n=0}^{N-1} x\left(m, n\right) e^{-j2\pi mk} e^{-j2\pi nl} \tag{8}$$

where $k = 0,\ 1/M,\ \ldots,\ M - 1/M$; $l = 0,\ 1/N,\ \ldots,\ N - 1/N$.

The corresponding inverse discrete Fourier transform (IDFT) for $X(k, l)$ is

$$x\left(m, n\right) = \frac{1}{MN}\sum_{k=0}^{M-1}\sum_{l=0}^{N-1} X\left(k, l\right) e^{j2\pi km} e^{j2\pi ln} \tag{9}$$

where $m = 0,\ 1/M,\ \ldots,\ M - 1/M$; $n = 0,\ 1/N,\ \ldots,\ N - 1/N$.

To take advantage of the efficiency of DFT/IDFT, we uniformly sample k_1, k_2 (in (6)) with K, L points ($K = 2^\mu \geq M$, $L = 2^\eta \geq N$; μ, η are positive integers) and pad the element excitations I by zero if necessary, then (6) equals

$$F_a\left(p, q\right) = \sum_{m=0}^{K-1}\sum_{n=0}^{L-1} I_{mn} \cdot e^{j2\pi(mp+nq)} \tag{10}$$

where

$$p = \frac{k_1 d_1 \hat{k}_1 \cdot \hat{d}_1}{2\pi} \quad q = \frac{k_2 d_2 \hat{k}_2 \cdot \hat{d}_2}{2\pi} \tag{11}$$

Obviously, (10) is similar to (9), i.e., the array factor can be calculated by a 2-D $K \times L$ points IDFT,

$$F_a = \mathrm{IDFT}\left(I\right) \tag{12}$$

According to the principle of pattern multiplication the array pattern E_r equals the array factor F_a multiplied by the element pattern F_e, i.e., $E_r = F_a \cdot F_e$, and on the contrary, the array factor F_a equals the array pattern E_r divided by the element pattern F_e, i.e., $F_a = E_r/F_e$. After obtaining the array pattern, the next is to compare the pattern with the prescribed target. All the samples which exceed the limitations are altered following the rule in (13).

$$\left|E_d\left(p,q\right)\right| = P_M\left|E_r\left(p,q\right)\right| = \begin{cases} \left(M_u\left(p,q\right)/Q\right)^{\zeta}, & M_u\left(p,q\right) < \left|E_r\left(p,q\right)\right| \\ \left|E_r\left(p,q\right)\right|, & M_l\left(p,q\right) \le \left|E_r\left(p,q\right)\right| \le M_u\left(p,q\right) \\ \left(M_l\left(p,q\right)\cdot Q\right)^{\zeta}, & \left|E_r\left(p,q\right)\right| < M_l\left(p,q\right) \end{cases} \tag{13}$$

where P_M is the positive projection operator; E_r is the normalized calculated pattern; E_d is the normalized modified pattern; M_u, M_l are the upper and lower limitations of the required pattern; $Q = 10\text{^}(1 - (iter/iter\_\max)^{\gamma})$; $iter$ is the iteration number; $iter\_\max$ is the maximum iteration number; ζ, γ are real quantities, called in the following "perturbation factors". The larger ζ and smaller γ could speed up the convergence speed of the algorithm.

Then a renewed set of element excitations can be obtained by the inverse computation of (12), i.e., a 2-D $K \times L$ points DFT performed on the modified array factor. The Fourier result consists of $K \times L$ samples, and only the former $M \times N$ samples are associated with the array aperture. Other element excitations outside the aperture are set to zero.

The procedure of the synthesis approach for periodic planar arrays can be summarized as:

1) Determine the wavenumber vectors $\hat{k}_1$, $\hat{k}_2$ according to Equation (5).
2) Design the upper and lower constraint target patterns M_u, M_l.
3) Calculate the array factor F_a (12) and the array pattern E_r.
4) Judge whether the iteration satisfies the terminate conditions, break or continue.
5) Modify the array pattern following the rule (13).
6) Calculate the renewed set of element excitations and only retain the samples within the aperture.
7) Back to step 3).

The synthesis approach is also suitable for constrained complex weighted problems. It just needs adding a modification procedure at the beginning of step 3). The modification on the element excitations was first given in detail in [18]. Until now, we have finished the synthesis in an affine coordinate system. While in practical engineering applications, one prefers to express the pattern in Cartesian or spherical coordinate. The available interp2 in Matlab can be employed to calculate the pattern samples one needs quickly, and the brute force method consisting of the summation of the individual contribution of each element to the far-field is also feasible.

During the synthesis process, the key is to design the upper and lower constraint target patterns in an affine coordinate system. In wavenumber space, the relationship between different wavenumber vectors is

$$k_1\hat{k}_1 + k_2\hat{k}_2 = k_x\hat{x} + k_y\hat{y} \tag{14}$$

If one performs scalar product on both sides of (14) with $\hat{d}_1$, $\hat{d}_2$, $\hat{x}$ and $\hat{y}$ successively and it satisfies $\hat{k}_1 \cdot \hat{d}_2 = 0$, $\hat{k}_2 \cdot \hat{d}_1 = 0$, then there will be the transformations

$$k_1 = \frac{k_x\hat{x}\cdot\hat{d}_1 + k_y\hat{y}\cdot\hat{d}_1}{\hat{k}_1\cdot\hat{d}_1} \quad k_2 = \frac{k_x\hat{x}\cdot\hat{d}_2 + k_y\hat{y}\cdot\hat{d}_2}{\hat{k}_2\cdot\hat{d}_2} \tag{15}$$

$$k_x = k_1\hat{k}_1\cdot\hat{x} + k_2\hat{k}_2\cdot\hat{x} \quad k_y = k_1\hat{k}_1\cdot\hat{y} + k_2\hat{k}_2\cdot\hat{y} \tag{16}$$

Since the upper and lower limitations of the target expressed by k_x, k_y (or u, v) in the Cartesian coordinate system are known to us, the values p, q corresponding to k_x, k_y in an affine coordinate can be calculated by (15) and (11). According to the minimum and maximum values of p, q, the Fourier intervals of the array factor (10) can be obtained, and then the sampling points k_1, k_2 (or p, q) of the array factor in an affine coordinate system are obtained. The values k_x, k_y corresponding to k_1, k_2 (or p, q) in the Cartesian coordinate could be calculated by (13). Therefore, the upper and lower constraint target patterns in an affine coordinate system are obtained.

Since DFT/IDFT can only deal with discrete quantities and to ensure accuracy, large Fourier sampling number is necessary. In our examples, 2-D 1024×1024 points FFTs were selected to calculate the array factor in an affine coordinate, and final 2-D 1025×1025 points were chosen to express the pattern in the Cartesian coordinate system.

4. SYNTHESIS RESULTS

Several examples have been performed on our personal computer with an Intel(R) Core(TM) i3 processor operating at 3.2 GHz and equipped with 2 GB RAM to verify the rationality of the proposed method. The perturbation factors ζ, γ are chosen as 0.5 and 2, respectively. For simplicity, the arrays were composed of isotropic elements. The initial element excitations were selected as one, and the synthesis problems were unconstrained complex weighted problems.

First, it was the synthesis of the array with a circular aperture with a diameter of 33.01-wavelength. The synthesis target was to obtain a pattern with a multilevel sidelobe performance. The requirements were: SLL (sidelobe level) ≤ -52 dB for the ring $\{0.076^2 < u^2 + v^2 \leq 0.3^2\}$, $SLL \leq -70$ dB for the ring $\{0.3^2 < u^2 + v^2 \leq 0.6^2\}$ and $SLL \leq -80$ dB for the ring $\{0.6^2 < u^2 + v^2 \leq 1^2\}$. Three experiments with different periodic element layouts were performed. As special cases, the square grid with $\alpha = 90°$, $\beta = 45°$ (case 1) and the equilateral triangle grid with $\alpha = 60°$, $\beta = 60°$ (case 2) were included, and a parallelogram grid with $\alpha = 50°$, $\beta = 60°$ (case 3) was also involved. The angles α, β are the inner angles of the triangle lattice which is shown in Figure 1. The element spacings d_1, d_2 (d_1, d_2 are the element spacings along the directions $\overrightarrow{d_1}$, $\overrightarrow{d_2}$ as shown in Figure 1) and total element number of these three cases are shown in Table 1. From the data shown in Table 1, it is clear that case 2 and case 3 have larger element spacings than case 1, and own a reduction about 13.12% and 16.64% in the element number.

Table 1. Element spacings and total element number.

Case		1	2	3
Element spacings	d_1/λ	0.5	0.5774	0.6015
	d_2/λ	0.5	0.5774	0.6527
Total element number		3413	2965	2845

The maximum iteration number was set to 8000. The synthesized results are shown in Table 2. To illustrate the generality of the alternating projection method in an affine coordinate system, the results obtained by the conventional and another modified projection operators were also added to the table. In our examples, the other modified projection operator was given briefly in [17], and the parameters m, n were chosen as 1 and 2.

From the results shown in Table 2, it can be noted that with the two modified projection operators, the iteration stopped with the pattern completely satisfied the requirements in an affine coordinate system for both cases 1, 2 and 3. For cases 2 and 3, the pattern satisfied the requirements completely in an affine coordinate system, while in the Cartesian coordinate system there were still samples exceeding the requirements. This is because DFT/IDFT can only deal with discrete quantities, and the sample wanted to be obtained in the Cartesian coordinate system does not always have a corresponding sample accurately calculated in the affine coordinate system. To ensure accuracy, one can only increase the Fourier sampling points. From the results shown in Table 2, it also can be observed that with the two modified projection operators, there were 20 and 34 (or 33) samples exceeding the requirements for case 2 and case 3 in the Cartesian coordinate system.

Table 2. Synthesized results of different projection operators.

Case	Projection operator	Iteration number	Unsatisfied sample	Computation time
1	conventional	8000	11492	2159 s
	[17]	625	0	179 s
	(13)	613	0	172 s
2	conventional	8000	3142	2560 s
	[17]	862	20	287 s
	(13)	800	20	260 s
3	conventional	8000	2966	2846 s
	[17]	882	33	333 s
	(13)	854	34	315 s

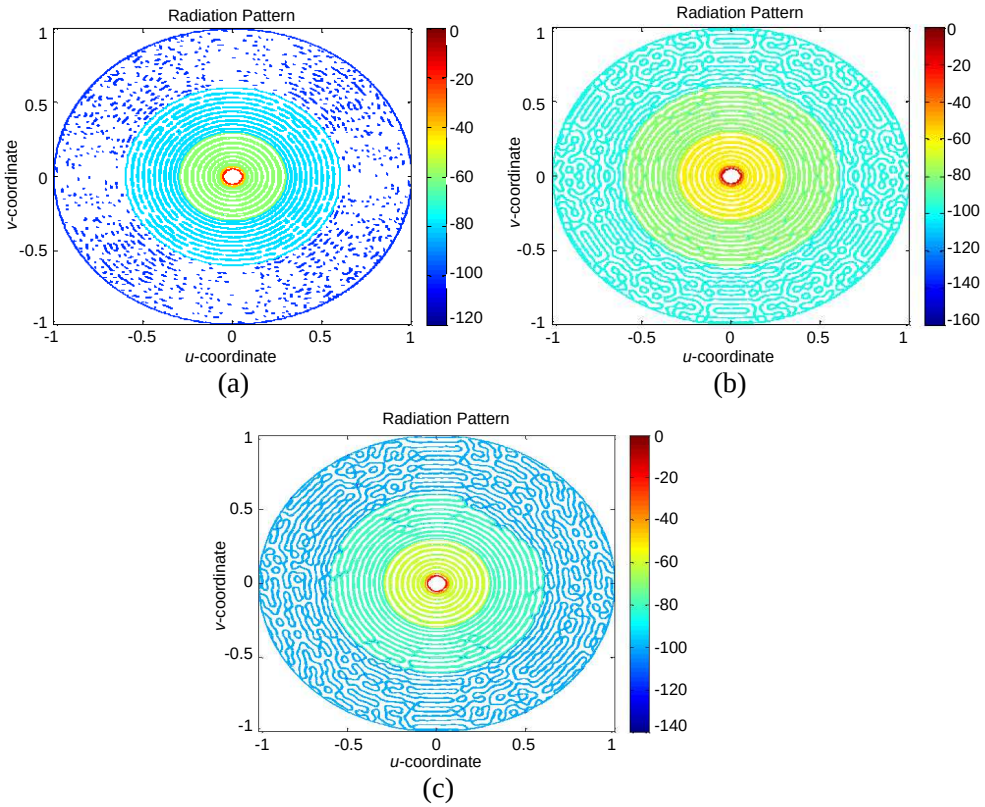

Figure 2. Contour plots of our synthesized patterns (measured in dB). (a) Case 1. (b) Case 2. (c) Case 3.

The contour plots of the synthesized patterns obtained by our proposed method are shown in Figure 2. The synthesized patterns had a same directivity of 37.99 dB. The aperture current distributions pertaining to the synthesized patterns are shown in Figure 3 with a taper efficiency of 0.5569, 0.5532 and 0.5490, respectively.

The u-cut and v-cut of the synthesized patterns through the main beam peak are shown in Figure 4. To illustrate the interpolation accuracy of interp2, the results obtained by direct summation are also added into the figures. The solid line plots the result obtained by interp2, and the dotted line plots the actual result calculated by direct summation.

Second, it was the synthesis of the array with elements placed on an equilateral triangle grid with $d_y = \lambda/2$ as shown in Figure 5. The array was composed of 28 concentric hexagonal rings and an

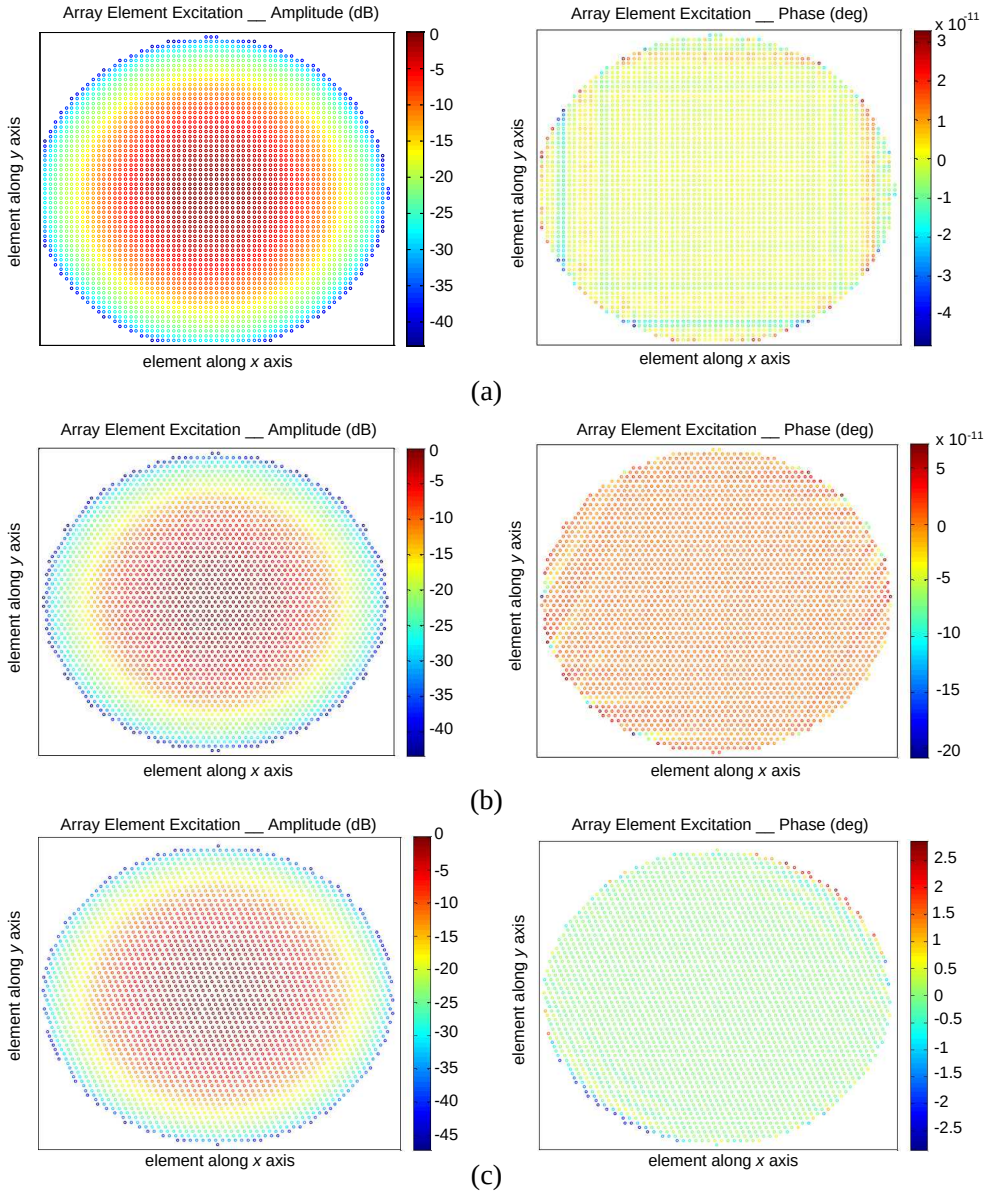

Figure 3. Aperture current distribution. (a) Case 1. (b) Case 2. (c) Case 3.

Table 3. Synthesized results of different projection operators.

Projection operator	Iteration number	Unsatisfied sample	Computation time
conventional	8000	32	2559 s
[17]	176	4	60 s
(13)	175	4	58 s

additional single element located at the center with a total element number of 2437.

The synthesis target was to achieve a pattern with a maximum sidelobe level of -55 dB for the ring $\{0.08^2 \leq u^2 + v^2 \leq 1\}$. The maximum iteration number was set to 8000. The synthesized results are shown in Table 3.

From the results shown in Table 3, it can be noted that the synthesis with the two modified projection operators had better results and required less computation time. The synthesized patterns

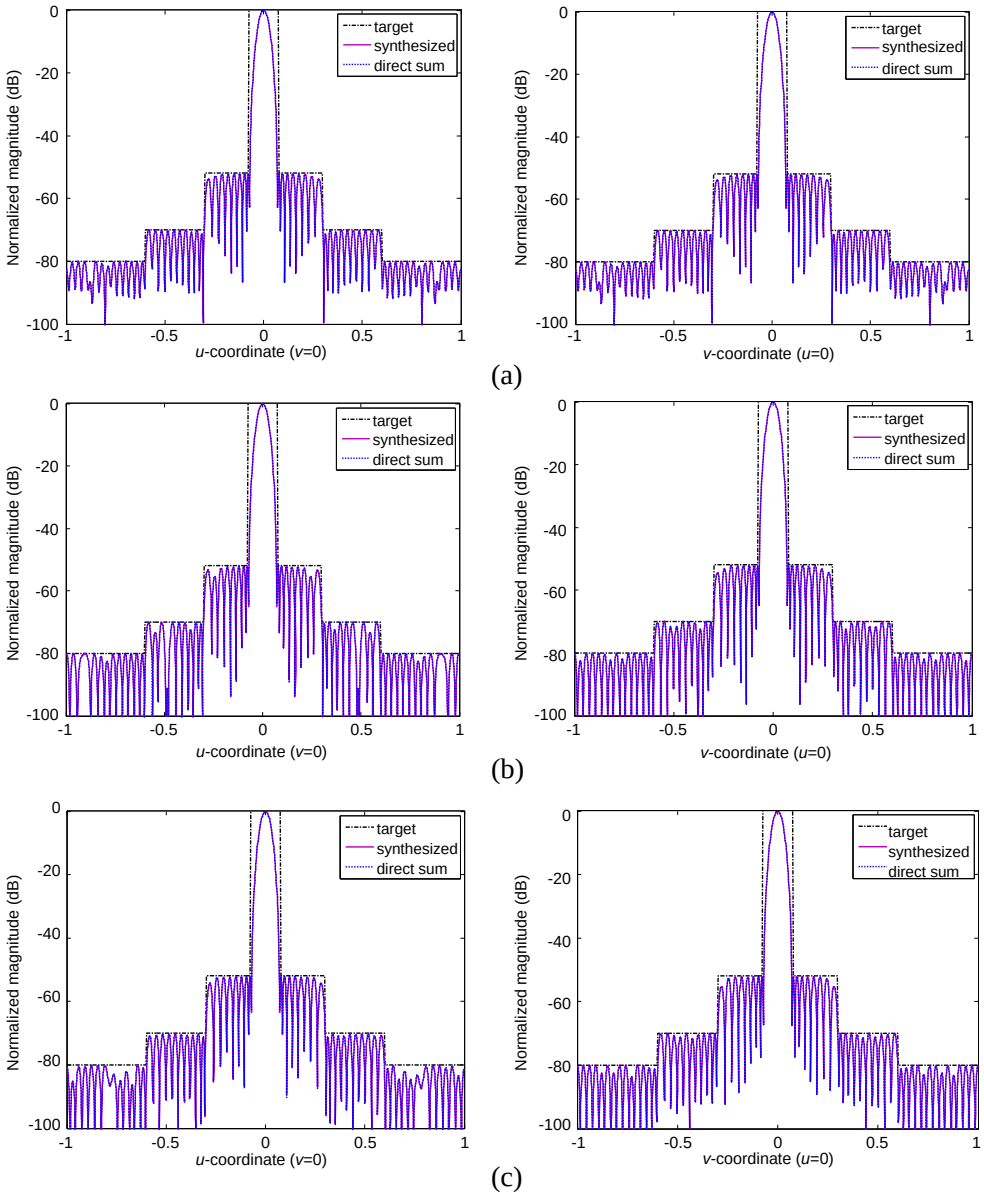

Figure 4. U-cut and v-cut of the synthesized patterns. (a) Case 1. (b) Case 2. (c) Case 3.

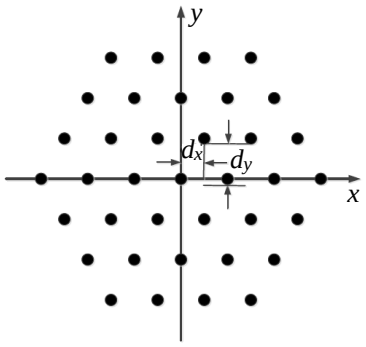

Figure 5. Geometry of the hexagonal planar array.

had four samples exceed the requirements. The magnitudes of these four samples were −54.91 dB, −54.91 dB, −54.88 dB, −54.88 dB and −54.94 dB, −54.94 dB, −54.89 dB, −54.89 dB with a maximum difference of 0.12 dB and 0.11 dB between the synthesized and required patterns for the synthesis with other and our modified projection operators.

Obviously, our synthesized pattern was a little better and required less computation time. The u-cut and v-cut of our synthesized pattern are shown in Figure 6. The pattern had a directivity of 37.21 dB with a taper efficiency of 0.5371. Figure 7 depicts the aperture current distribution pertaining to the pattern.

Third, it was the synthesis of the array which had the same element layout as case 3 in the first example, featuring an approximate square aperture with a side length of 33.01-wavelength. The antenna number was 3677. Compared with the array with a square element layout as case 1 in the first example (the element number required was 4489 in this case), it has a reduction about 18.09% in the element number. The synthesis target was to obtain a pattern with three flat sectors and three nulled sectors.

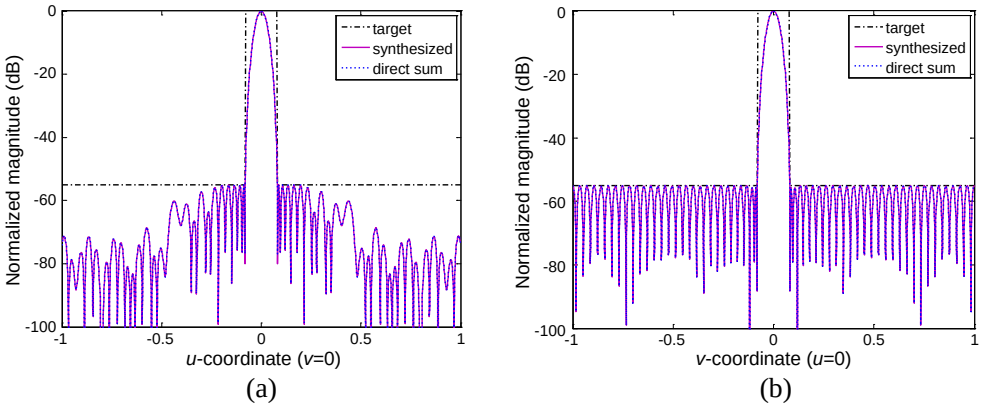

Figure 6. Our synthesized radiation pattern. (a) U-cut. (b) V-cut.

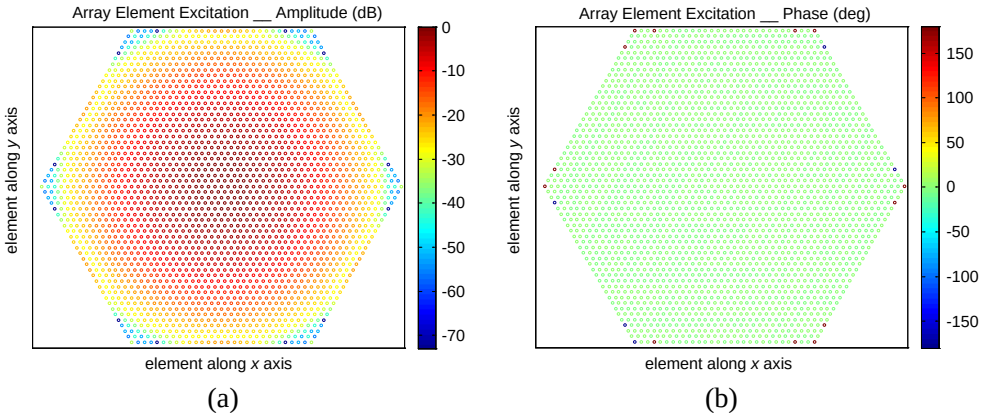

Figure 7. Aperture distribution pertaining to our synthesized pattern. (a) Amplitude. (b) Phase.

Table 4. Constraint regions and SLL limitations.

constraint region	SLL limitation
$0.05^2 \le u^2 + v^2 \le 0.3^2$	≤ -35 dB
$0.3^2 < u^2 + v^2 \le 0.6^2$	≤ -40 dB
$0.6^2 < u^2 + v^2 \le 1$	≤ -50 dB
$-0.8 \le u \le -0.7$; $-0.3 \le v \le 0.1$	≤ -58 dB
$-0.2 \le u \le 0.15$; $0.4 \le v \le 0.55$	≤ -60 dB
$0.4 \le u \le 0.5$; $-0.3 \le v \le 0.1$	≤ -62 dB

Table 5. Synthesized results of different projection operators.

Projection operator	Iteration number	Unsatisfied sample	Computation time
conventional	8000	90	2846 s
[17]	401	89	153 s
(13)	385	90	143 s

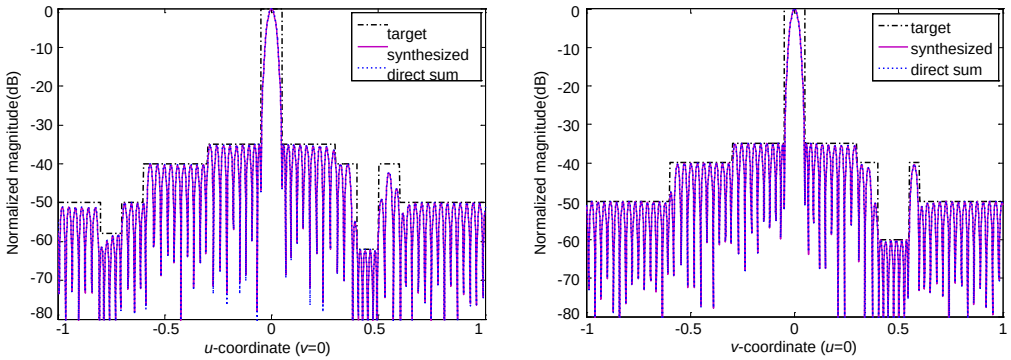

Figure 8. Our synthesized radiation pattern. (a) U-cut. (b) V-cut.

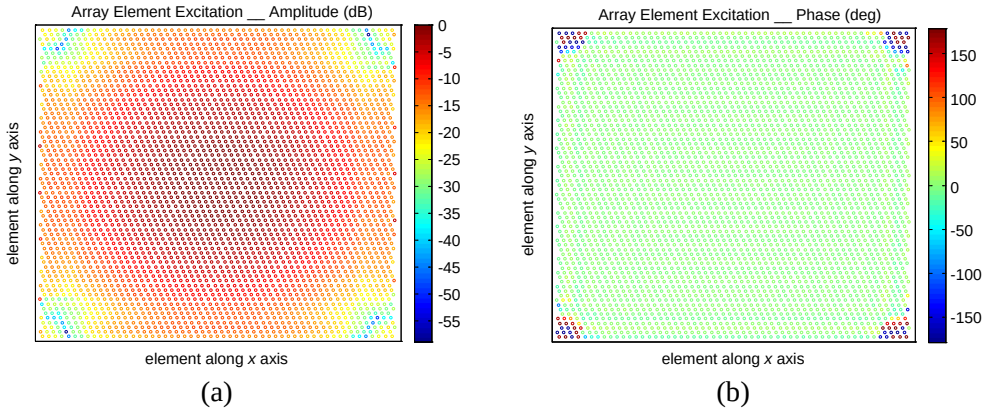

Figure 9. Aperture distribution pertaining to the synthesized pattern. (a) Amplitude. (b) Phase.

The corresponding constraint regions and sidelobe level (SLL) limitations are shown in Table 4.

The maximum iteration number was set to 8000. The synthesized results of different projection operators are shown in Table 5. From the results, it can be noted that the synthesized patterns had 90, 89 and 90 samples exceeding the requirements and our computation time was the least. Figure 8 depicts the u-cut and v-cut of the synthesized pattern through the main beam peak. The pattern had a directivity of 40.07 dB with a taper efficiency of 0.6739. Figure 9 depicts the aperture current distribution pertaining to the synthesized pattern.

From the depicted patterns above (Figures 4, 6 and 8), it can be noted that the results obtained by interp2 were almost the same as the actual value calculated by direct summation.

5. CONCLUSION

A pattern synthesis approach based on the alternating projection method in an affine coordinate system is presented. It is suitable for large planar arrays with periodic element layouts (rectangle, triangle and parallelogram). The proposed method with a modified projection operator in an affine coordinate system can synthesize the array pattern to the required with fast convergence rate and high accuracy. In addition, if the array has elements placed on a triangle or parallelogram grid, the reductions in the

number of the antenna elements and other associated components provide the designer lighter weight and lower manufacturing cost.

REFERENCES

1. Sharp, E. D., "A triangular arrangement of planar-array elements that reduces the number needed," *IRE Transactions on Antennas and Propagation*, Vol. 9, No. 2, 126–129, 1961.
2. Lo, Y. T. and S. W. Lee, "Affine transformation and its application to antenna arrays," *IEEE Transactions on Antennas and Propagation*, Vol. 13, No. 6, 890–896, 1965.
3. Han, J. H., S. H. Lim, and N. H. Myung, "Array antenna TRM failure compensation using adaptively weighted beam pattern mask based on genetic algorithm," *IEEE Antennas and Wireless Propagation Letters*, Vol. 11, 18–21, 2012.
4. Cen, L., Z. L. Yu, W. Ser, et al., "Linear aperiodic array synthesis using an improved genetic algorithm," *IEEE Transactions on Antennas and Propagation*, Vol. 60, No. 2, 895–902, 2012.
5. Ismail, T. H. and Z. M. Hamici, "Array pattern synthesis using digital phase control by quantized particle swarm optimization," *IEEE Transactions on Antennas and Propagation*, Vol. 58, No. 6, 2142–2145, 2010.
6. Wang, W. B., Q. Y. Feng, and D. Liu, "Synthesis of thinned linear and planar antenna arrays using binary PSO algorithm," *Progress In Electromagnetics Research*, Vol. 127, 371–387, 2012.
7. Bai, Y. Y., S. Q. Xiao, C. R. Liu, et al., "A hybrid IWO/PSO algorithm for pattern synthesis of conformal phased arrays," *IEEE Transactions on Antennas and Propagation*, Vol. 61, No. 4, 2328–2332, 2013.
8. Yang, J., W. T. Li, X. W. Shi, et al., "A hybrid ABC-DE algorithm and its application for time-modulated arrays pattern synthesis," *IEEE Transactions on Antennas and Propagation*, Vol. 61, No. 11, 5485–5495, 2013.
9. Keizer, W. P. M. N., "Fast low-sidelobe synthesis for large planar array antennas utilizing successive fast Fourier transforms of the array factor," *IEEE Transactions on Antennas and Propagation*, Vol. 55, No. 3, 715–722, 2007.
10. Keizer, W. P. M. N., "Element failure correction for a large monopulse phased array antenna with active amplitude weighting," *IEEE Transactions on Antennas and Propagation*, Vol. 55, No. 8, 2211–2218, 2007.
11. Keizer, W. P. M. N., "Large planar array thinning using iterative FFT techniques," *IEEE Transactions on Antennas and Propagation*, Vol. 57, No. 10, 3359–3362, 2009.
12. Wang, X. K., Y. C. Jiao, and Y. Y. Tan, "Synthesis of large thinned planar arrays using a modified iterative Fourier technique," *IEEE Transactions on Antennas and Propagation*, Vol. 62, No. 4, 1564–1571, 2014.
13. Bucci, O. M., G. Franceschetti, G. Mazzarella, et al., "Intersection approach to array pattern synthesis," *IEE Proceedings H, on Microwaves, Antennas and Propagation*, Vol. 137, No. 6, 349–357, 1990.
14. Bucci, O. M., G. D. Elia, G. Mazzarella, et al., "Antenna pattern synthesis: A new general approach," *Proceedings of the IEEE*, Vol. 82, No. 3, 358–371, 1994.
15. Trincia, D., L. Mareaccioli, R. V. Gatti, et al., "Modified projection method for array pattern synthesis," *IEEE 34th European Microwave Conference*, 1397–1400, Amsterdam, Netherlands, Oct. 2004.
16. Quijano, J. L. A. and G. Vecchi, "Alternating adaptive projections in antenna synthesis," *IEEE Transactions on Antennas and Propagation*, Vol. 58, No. 3, 727–737, 2010.
17. Han, D. D., W. Wu, and B. Du, "Perturbation alternating projections method for pattern synthesis of phased array antenna," *IEEE Global Symposium on Millimeter Waves (GSMM)*, 385–388, Harbin, China, May 2012.
18. Franceschetti, G., G. Mazzarella, and G. Panariello, "Array synthesis with excitation constraints," *IEEE Antennas and Propagation Society International Symposium*, 1192–1195, Jun. 1988.